JOURNAL OF AGRICULTURAL AND FOOD CHEMISTRY

Postharvest Ripening Study of Sweet Lime (*Citrus limettioides*) in Situ by Volume-Localized NMR Spectroscopy

ABHISHEK BANERJEE, CHRISTY GEORGE, SATHYAMOORTHY BHARATHWAJ, AND NARAYANAN CHANDRAKUMAR*

Department of Chemistry, Indian Institute of Technology—Madras, Chennai 600036, Tamil Nadu, India

Spatially resolved NMR—especially volume-localized spectroscopy (VLS)—is useful in various fields including clinical diagnosis, process monitoring, etc. VLS carries high significance because of its ability to identify molecular species and hence track molecular events. This paper reports the application of VLS at 200 MHz to study the postharvest ripening of sweet lime (*Citrus limettioides*) in situ, including a comparative study of normal and acetylene-mediated ripening. Localization to a cubic voxel of 64 μL was achieved with point-resolved spectroscopy (PRESS). Glucose, sucrose, fructose, and citric acid are found to be among the main constituents in the fruit. In the natural process, the sugar to acid ratio increases with ripening. Ethanol generation is seen to occur at a faster rate in acetylene-mediated ripening. Whereas NMR imaging experiments including parametric imaging (e.g., T_1 or T_2 maps) may be employed for "macro" monitoring of processes such as these, this work demonstrates that the molecular imprint of the process may be tracked noninvasively by VLS.

KEYWORDS: ***Citrus limettioides*; ripening; acetylene; volume-localized spectroscopy; PRESS**

INTRODUCTION

Citrus limettioides (sweet lime) is a fruit that is widely used in tropical America, Italy, and parts of India. It is used for its cooling effects in cases of jaundice or high fever, and its juice is used as a sweet drink in summer. Taste development in ripened fruits is due to various molecular changes occurring during the ripening process. The ripening hormone ethylene initiates the action of various endogenous hormones, resulting in the breakdown of chlorophyll, hydrolysis of polysaccharides to sugar, and decrease in acidity (*1*). It is reported from high-resolution NMR studies in vitro on mango fruit extracts that the sugar to acid ratio and the content of minor components such as ethanol and α-alanine also increase as the fruit ripens (*2*).

Fruits are classified as climacteric and nonclimacteric depending on their postharvest ripening behavior. Climacteric fruits show an increase in respiration rate and a sudden increase in ethylene biosynthesis at the onset of ripening. Such changes are absent in nonclimacteric fruits, which are incapable of postharvest ripening. However, some nonclimacteric fruits are reported to show a response to ethylene if supplied artificially. Citrus fruits belong to this particular category (*1, 3*).

External application of ethylene is the standard method for artificial ripening. Use of carbides is another commonly practiced method, and here the acetylene generated from the carbide is the actual stimulant for ripening. However, this method is reported to be harmful to the body (*4, 5*). Earlier works on fruit ripening at the molecular level were done by the extraction of the fruit juice or its constituents and subsequent analysis by HPLC or spectroscopy (*2, 6*−*11*). These methods are destructive in nature and open to questions of reliability because of the possible chemical transformations and contamination during extraction and analysis. Other nondestructive studies have been reported, which concentrate mainly on the textural modifications in the fruit due to ripening by NMR T_1, T_2, or diffusion mapping. It has generally been observed that molecular events are not unequivocally reflected in such relaxometric and diffusometric studies (*12*−*17*).

We show here that spatially resolved NMR—especially volume-localized spectroscopy (VLS) (*18*−*22*)—is an efficient nondestructive tool in the study of fruit ripening that tracks molecular events. Because VLS is completely noninvasive, it gives reliable results and helps us to track and understand the ripening process at the molecular level. The present work is a comparison of the effect of natural and artificial (acetylene mediated) ripening on the molecular constituents of the harvested fruit of *C. limettioides*.

MATERIALS AND METHODS

Studies were carried out with the nonclimacteric fruit, *C. limettioides* (sweet lime). Fresh, clean green-skinned fruits were procured from the local market and used without further processing. For the comparative study of natural and artificial ripening, sets of three fruits were selected in each case. In the natural ripening case fruits were stored at room

* Corresponding author (e-mail nckumar@iitm.ac.in).

10.1021/jf803159u CCC: $40.75
Published on Web 01/22/2009

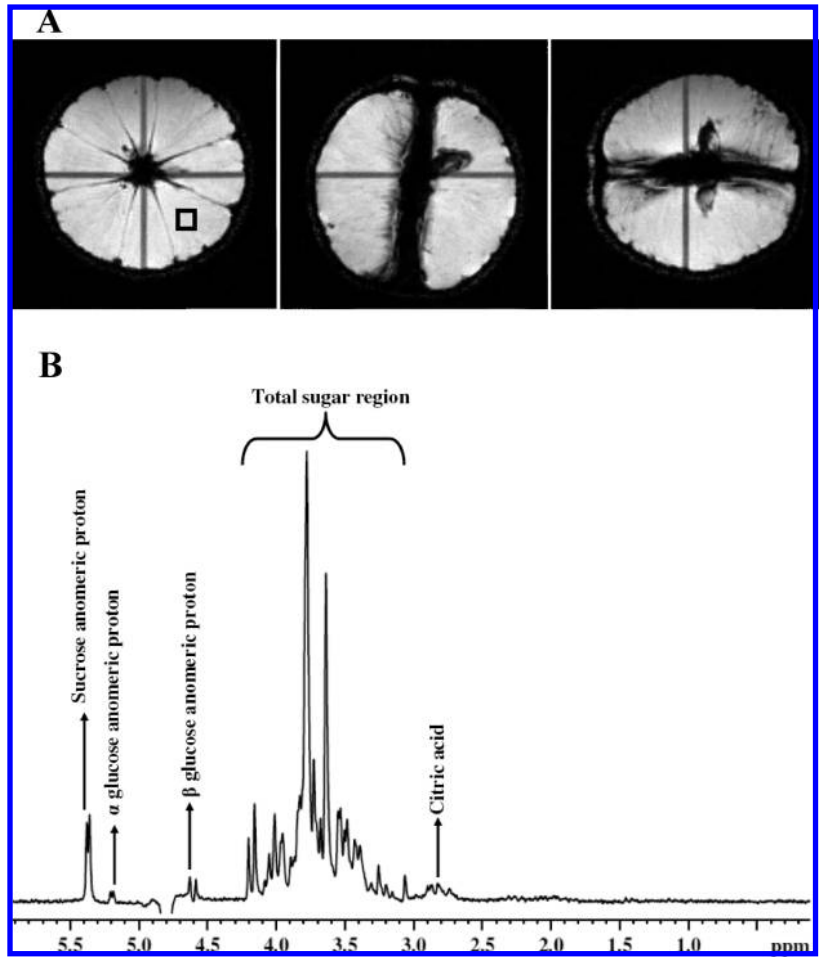

Figure 1. (**A**) Gradient echo images collected with a matrix size of 128 × 128: echo time, 6 ms; repetition time, 100 ms; slice thickness, 2 mm; FOV, 8 cm. (**B**) Spectrum obtained from a 4 mm voxel (marked with a square in the first image of (A)) of a sweet lime at the green-skinned stage.

temperature (ca. 23 °C). Artificial ripening was induced by acetylene generated in situ from crude calcium carbide (5−10 g) inside a desiccator containing the fruits.

Experiments were carried out on a Bruker BIOSPEC 200 MHz 47/40 MRI system employing a 7.2 cm i.d. ^{1}H resonator. Volume localization was achieved by the double-spin−echo point-resolved spectroscopy (PRESS) sequence. A set of gradient echo images were taken along the three different orientations, axial, coronal, and sagittal, and voxel selection was done with the help of multislice imaging along these three directions. A total of 32−36 images were taken along each of the three orientations, with a slice thickness and interslice distance each of 2 mm. A 4 × 4 × 4 mm^3 voxel was selected in a homogeneous portion of the fruit. Magnetic field homogeneity was optimized over the voxel by employing the Fastmap algorithm. Whenever possible, the same voxel was used for measurements over the course of weeks. Because the water proton concentration is of the order of 110 M, highly efficient suppression of the water signal is essential to observe the molecular constituents present in the fruit. This was achieved by chemical shift selective saturation (CHESS). For the close-lying signals of the anomeric protons of glucose and sucrose to be measured with a degree of reliability, the CHESS suppression bandwidth was optimized to 40 Hz. Whereas the variable pulse power and optimized relaxation delay (VAPOR) water suppression technique is arguably more efficient, a tradeoff against selectivity seems to come into play; this suppression scheme was therefore not our method of choice. All spectra were taken with 512 scans using a repetition time of 1550.83 ms and an echo time of 20 ms. The total experiment time to collect the spectrum was 13 min and 20 s. All spectra were acquired with 2K complex data points in PARAVISION (corresponding to TD = 4K in TOPSPIN), and the spectral width was 10 ppm. The time domain data were zero filled to 8K points in TOPSPIN (corresponding to 4K complex points in PARAVISION), and an LB of 0.5 was used for further processing prior to Fourier transformation without any truncation artifacts. Measurements were carried out at different time periods over a month to monitor the changes in the molecular constituents of the fruit.

RESULTS AND DISCUSSION

The gradient echo images obtained from the fruit along three perpendicular axes are shown in **Figure 1A**. These pilot images help visualize the internal structure of the fruit. Fruits that had any visible damage or air gaps in the flesh were discarded.

Figure 1B shows a representative spectrum obtained from the sweet lime at the stage it was collected from the market. Glucose, sucrose, and citric acid peaks are well resolved in the spectrum. The chemical shift axis of the spectrum is calibrated with respect to the suppressed water peak at 4.8 ppm. The main sugar contribution is observed in the 3.0−4.3 ppm range. This region contains peaks due to different sugars present in the fruit, mainly sucrose, α-glucose, β-glucose, and fructose. In addition to this, some of the ethanol and α-alanine peaks occur in this range. The anomeric proton of sucrose appears at 5.4 ppm, whereas peaks at 5.25 and 4.62 ppm are due to the anomeric protons of α-glucose and β-glucose, respectively. Citric acid peaks appear at 2.85 ppm as a relatively broad multiplet. Two minor peaks at 1.14 and 1.43 ppm, which are discernible at later stages of ripening, are due respectively to methyl protons of ethanol and α-alanine. The $-CH_2$ and $-CH$ proton peaks from these molecules—as well as other possible species—come within the main sugar region and may only be distinguished by suitable spectral editing for complete assignment. Instead, we have adopted the simpler "mix and match" strategy of employing

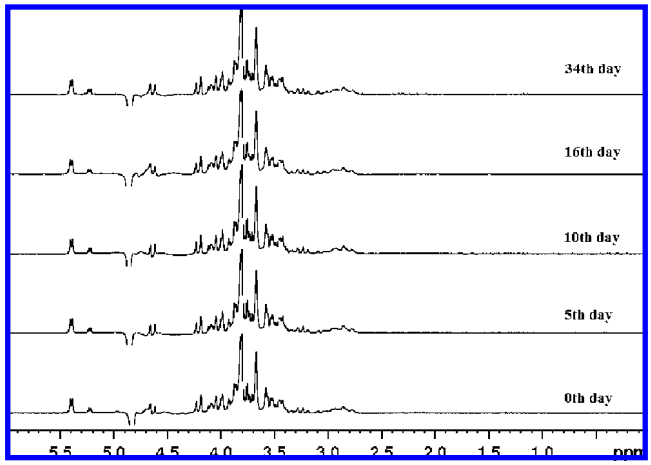

Figure 2. Spectra obtained from a representative sample in the natural ripening case as a function of time.

a model solution having a spectrum that is in close accord with the fruit spectrum down to the 5 mM level (vide infra). It may be noted that a selective suppression sequence such as CHESS with a bandwidth of ca. 40 Hz enables visualization of peaks just 36 Hz away from the water signal. Even under this condition, however, these peaks lying very close to water will be affected by the suppression pulses, and the actual intensities would be more than the observed intensity, especially in the case of the anomeric doublet at 4.62 ppm.

From the literature it is clear that, as the fruit ripens, the sugar to acid ratio and the ethanol and α-alanine contents, etc., increase (*2*). Hence, these parameters give us a clear idea about the state of ripening of the fruit as a function of time. In our studies increase in the sugar to acid ratio is considered as the primary evidence of ripening and is monitored quantitatively from the peak areas corresponding to sugar and acid. The sugar to acid ratio is calculated both from the major sugar region (3−4.3 ppm) and from the sucrose anomeric proton signal (5.4 ppm) and α-glucose anomeric proton signal (5.25 ppm), relative to the acid region (2.6−3 ppm). The *β*-glucose anomeric peak is too close to the water peak to permit accurate quantitation. The peaks at 5.4 and 5.25 ppm are specific imprints of sucrose and α-glucose anomeric protons, respectively, and hence the anomeric sugar to acid ratio gives molecule-specific information. The 3−4.3 ppm region contains contributions from various sugars and shows the change in total sugar concentration, including the contribution of fructose.

Natural Ripening. Three different fruits (samples 1, 2, and 3) were used for these studies. **Figure 2** shows a representative set of spectra obtained as a function of time in the natural ripening case. (The corresponding data for the acetylene-mediated case are shown in **Figure 3**.) The triplet at 1.14 ppm, assigned to the methyl protons of ethanol, shows an increase in intensity as a function of time. This peak is almost unobservable at the earlier stages of ripening, and its increase in intensity as a function of time is a confirmation of the fact that ethanol concentration increases as the fruit ripens. **Figure 4** (NR1) depicts the sugar (3−4.3 ppm region) to acid (2.6−3 ppm) ratio. The sucrose anomeric proton to acid ratio and α-glucose anomeric proton to acid ratio are both calculated and also shown in **Figure 4** (NR2 and NR3). The sugar to acid ratio shows a clear, although not monotonic, increase as the fruit ripens, as seen from the end points in the graphs in **Figure 4** (NR1, NR2, and NR3). The result is confirmed on three different fruits (samples 1, 2, and 3).

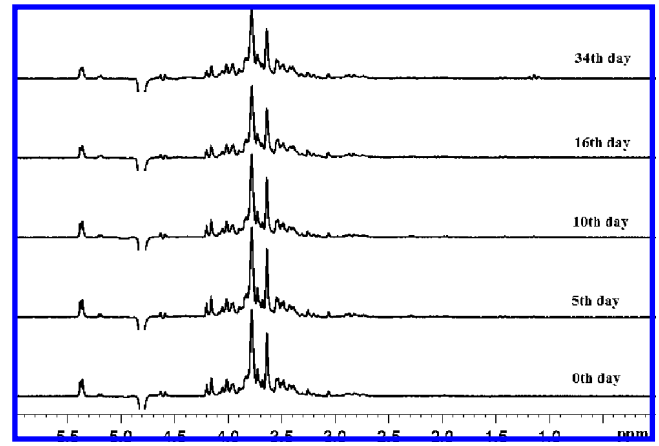

Figure 3. Spectra obtained from a representative sample in the acetylene-mediated case as a function of time. The spectrum on the 0th day refers to a measurement before the start of the acetylene treatment; subsequent *n*th day spectra therefore refer to *n* days of acetylene treatment. (The same "day numbering" convention has been adopted for **Figure 2** as well, but without implicating acetylene.)

Acetylene-Mediated Ripening. Three different fruits (samples 4, 5, and 6) were used for these studies. **Figure 3** shows the time course of spectra obtained from a representative sweet lime sample in the case of acetylene-mediated ripening. The sugar to acid ratio is calculated, as before, from the sucrose and glucose anomeric regions as well as the major sugar range, relative to the citric acid range. As ripening progresses, this ratio is found to increase after an initial dip, but eventually tends to stay below the initial value. This is clear from the graphs in **Figure 4** (AR1, AR2, and AR3). On the other hand, the increase in ethanol is much more prominent in the acetylene-mediated case than in the case of natural ripening, as is clear from **Figure 5**. The faster increase in ethanol may be attributed to a faster ripening of the fruit. In addition to this, visual inspection shows the skin of the fruit becomes yellow at a faster rate. These observations are in good agreement with the literature report that acetylene treatment causes quick ripening of the fruits by initiation of enzymatic activity, which causes the breakdown of sugars (*23*). During acetylene treatment it gets incorporated into the fruit and is harmful to the human body (*24*). Indeed, in some specimens treated with higher concentrations of carbide the acetylene peak could be detected at 2.27 ppm in the volume-localized spectra (not shown here).

Model Solution Study. The absolute concentrations of various molecular constituents of the fruit were measured from experiments on a phantom, containing a suitably constituted model solution. A model solution containing sucrose, fructose (110 mM each), glucose (65 mM), citric acid (55 mM), α-alanine (10 mM), ethanol (25 mM), methanol (37 mM), and choline hydroxide solution (20 mM) resulted in a spectrum that closely resembled the fruit voxel spectrum (except for the methanol and choline peaks, which were then scaled appropriately). The volume-localized spectrum of the model solution was acquired with the identical set of parameters that were employed for the fruit experiments. The sugar peaks show a one-to-one correspondence in the fruit and model solution spectra as seen from **Figure 6**; their linewidths are also comparable. However, the citric acid peaks in the fruit occur as a broad multiplet, as against a highly resolved set of four lines in the model solution. This may be due to the association of citric acid with fruit tissues and/or complex formation with the metal ions present in the fruit (*10*). The estimated concentration of various constituents present in the fruit, based on the

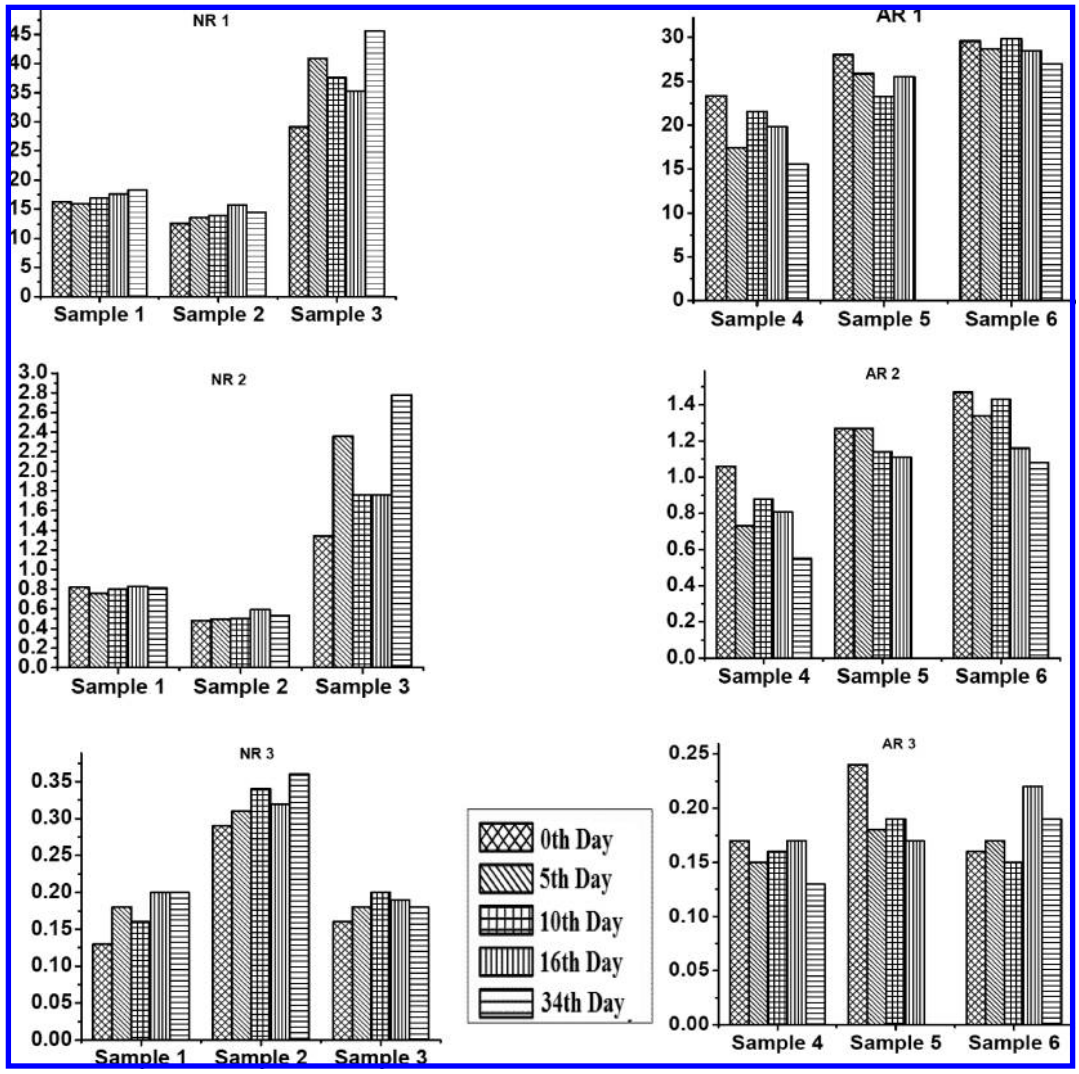

Figure 4. Bar chart representation of relevant molecular concentration ratios. The sugar to acid ratio shows an increase with time—although not monotonic—in the natural ripening (NR) study; in the acetylene-mediated (AR) ripening study, this ratio first dips and then rises, but tends to end up lower than at the start. (1) Ratio of the peak areas, 3.0−4.3 ppm to 2.6−3.0 ppm; (2) anomeric sucrose to acid ratio; (3) α-glucose to acid ratio.

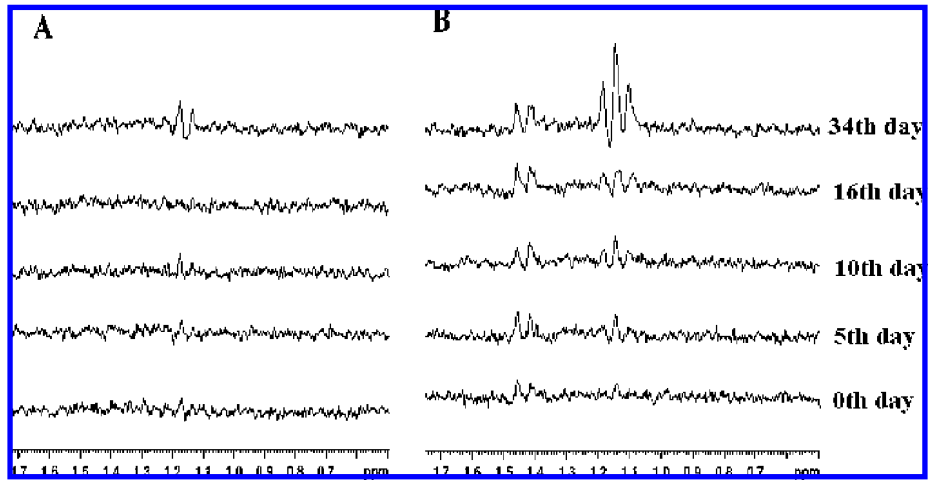

Figure 5. Spectra obtained from representative samples in the natural ripening (**A**) and acetylene-mediated ripening (**B**) cases as a function of time. Ethanol generation—and by implication the ripening process—occurs at a faster rate in the acetylene-mediated case.

comparison with the phantom studies, is given in **Table 1**. The singlet observed at 3.08 ppm is expected to be from choline (*2, 10*). However, the choline peak in the model solution is slightly shifted and merges with the high-field component of the glucose triplet at 3.14 ppm.

The goodness of the fit of the model solution spectrum with the fruit spectrum was directly estimated by calculating the difference spectrum of the two and resulted in a good null, except in the citric acid region; for the latter case, the integrals were compared in the relevant region and found to match.

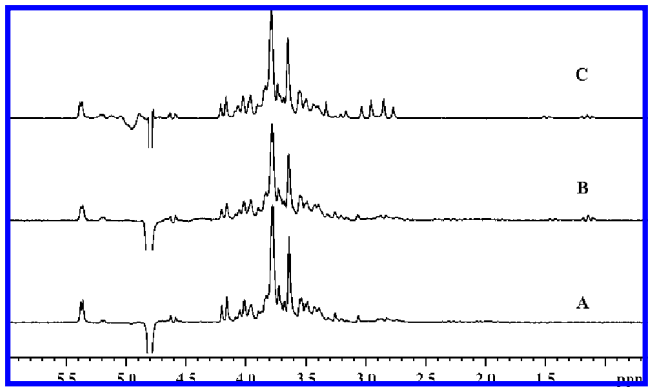

Figure 6. Comparison of fruit spectrum with model solution spectrum: (**A**) fruit spectrum at the initial stage (0th day) of ripening in the acetylene-mediated ripening study; (**B**) fruit spectrum at the final stage (34th day) of ripening in the acetylene-mediated case; (**C**) model solution spectrum.

Table 1. Range of Concentrations of Various Molecules Present in the Fruit

molecule	concentration (mM)
sucrose	110–120
glucose	65–70
fructose	110
citric acid	55
α-alanine[a]	10
ethanol[a]	25–30
choline	20
methanol	5–10

[a] At the completely ripened stage in the acetylene-mediated case.

Furthermore, it is gratifying to note that the predicted anomeric (5.25 and 5.4 ppm) to total sugar region (3−4.3 ppm) intensity ratio based on the model solution concentrations and glucose mutarotation equilibrium constant matched the experimental value on the fruit to considerably better than 1%.

The additional circumstance that the total sugar region (3−4.3 ppm) intensity predicted from the fruit spectrum anomeric region (5.25 and 5.4 ppm) intensity (based on the count of observable nonanomeric protons of sucrose and glucose, the glucose mutarotation equilibrium constant, and the fructose estimate from the model solution) deviated from the value observed in the fruit by +4% lends strong support to the inference that other possible constituents in the total sugar region, such as malic acid and aspartic acid, are below the detection threshold of ca. 5 mM.

In summary, volume-localized NMR spectral measurements clearly prove to be a potent technique in the in situ monitoring of fruit ripening at the molecular level.

LITERATURE CITED

(1) Prasanna, V.; Prabha, T. N.; Tharanathan, R. N. Fruit ripening phenomena—an overview. *Crit. Rev. Food Sci. Nutr.* **2007**, *47*, 1–19.

(2) Gil, A. M.; Durate, I. F.; Delgadillo, I.; Colquhoun, I. J.; Casuscelli, F.; Humpfer, E.; Spraul, M. Study of the compositional changes of mango during ripening by use of nuclear magnetic resonance spectroscopy. *J. Agric. Food Chem.* **2000**, *48*, 1524–1536.

(3) Giovannoni, J. Molecular biology of fruit maturation and ripening. *Annu. Rev. Plant Physiol. Plant Mol. Biol.* **2001**, *52*, 725–749.

(4) Pal, R. K. Influence of ethrel and calcium carbide on respiration rate, ethylene evolution, electrolyte leakage and firmness of 'Dashehri' mango (*Mangifera indica*). *Indian J. Agric. Sci.* **1998**, *68* (4), 201–203.

(5) Pal, R. K. Ripening and rheological properties of mango as influenced by ethrel and calcium carbide. *J. Food Sci. Technol.* **1998**, *35* (4), 358–360.

(6) Albertini, M. V.; Carcouet, E.; Pailly, O.; Gambotti, C.; Luro, F.; Berti, L. Changes in organic acids and sugars during early stages of development of acidic and acidless citrus fruit. *J. Agric. Food Chem.* **2006**, *54*, 8335–8339.

(7) Raffo, A.; Gianferri, R.; Barbieri, R.; Brosio, E. Ripening of banana fruit monitored by water relaxation and diffusion ^{1}H-NMR measurements. *Food Chem.* **2005**, *89*, 149–158.

(8) Fort, D. A.; Swatloski, R. P.; Moyna, P.; Rogers, R. D.; Moyna, G. Use of ionic liquids in the study of fruit ripening by high-resolution ^{13}C NMR spectroscopy: 'green' solvents meet green bananas. *Chem. Commun.* **2006**, 714–716.

(9) Belton, P. S.; Delgadillo, I.; Holmes, E.; Nicholls, A.; Nicholson, J. K.; Spraul, M. Use of high-field ^{1}H NMR spectroscopy for the analysis of liquid foods. *J. Agric. Food Chem.* **1996**, *44*, 1483–1487.

(10) Sobolev, A. P.; Segre, A.; Lamanna, R. Proton high-field NMR study of tomato juice. *Magn. Reson. Chem.* **2003**, *41*, 237–245.

(11) Bennett, A. B.; Smith, G. M.; Nichols, B. G. Regulation of climacteric respiration in ripening avocado fruit. *Plant Physiol.* **1987**, *83*, 973–976.

(12) Létal, J.; Jirák, D.; Suderlová, L.; Hájek, M. MRI 'texture' analysis of MR images of apples during ripening and storage. *Lebensm.-Wiss. -Technol.* **2003**, *36*, 719–727.

(13) Galed, G.; Fernández-Valle, M. E.; Martínez, A.; Heras, A. Application of MRI to monitor the process of ripening and decay in citrus treated with chitosan solutions. *Magn. Reson. Imaging* **2004**, *22*, 127–137.

(14) Clark, C. J.; Drummond, L. N.; MacFall, J. S. Quantitative NMR imaging of kiwifruit (*Actinidia deliciosa*) during growth and ripening. *J. Sci. Food Agric.* **1998**, *78*, 349–358.

(15) Williamson, B.; Goodman, B. A.; Chudek, J. A. Nuclear magnetic resonance (NMR) micro-imaging of ripening red raspberry fruits. *New Phytol.* **1992**, *120*, 21–28.

(16) Clark, C. J.; MacFall, J. S. Quantitative magnetic resonance imaging of 'Fuyu' persimmon fruit during development and ripening. *Magn. Reson. Imaging* **2003**, *21*, 679–685.

(17) Clark, C. J.; Hockings, P. D.; Joyce, D. C.; Mazucco, R. A. Application of magnetic resonance imaging to pre- and post-harvest studies of fruits and vegetables. *Postharvest Biol. Technol.* **1997**, *11*, 1–21.

(18) Bottomley, P. A. Spatial localization in NMR spectroscopy in vivo. *Ann. N.Y. Acad. Sci.* **1987**, *508*, 333–348.

(19) Granot, J. Selected volume excitation using stimulated echoes (VEST). Applications to spatially localized spectroscopy and imaging. *J. Magn. Reson.* **1986**, *70*, 488–492.

(20) Kimmich, R.; Hoepfel, D. Volume-selective multipulse spin−echo spectroscopy. *J. Magn. Reson.* **1987**, *72*, 379–384.

(21) Ernst, T.; Hennig, J. Improved water suppression for localized in vivo ^{1}H spectroscopy. *J. Mag. Reson. B* **1995**, *106*, 181–186.

(22) Haase, A.; Frahm, J.; Matthaei, D.; Hänicke, W.; Merboldt, K.-D. FLASH imaging. Rapid NMR imaging using low flip-angle pulses. *J. Magn. Reson.* **1986**, *67*, 258–266.

(23) González-Aguilar, G. A.; Buta, J. G.; Wang, C. Y. Methyl jasmonate reduces chilling injury symptoms and enhances color development of 'Kent' mangoes. *J. Sci. Food Agric.* **2001**, *81*, 1244–1249.

(24) Delpierre, M. Manuel de laboratoire de analyses des dentees alimentaires. Rapport interne. *FAO-ITA* **1974**, *74*, 12–15.

Received for review October 10, 2008. Revised manuscript received December 16, 2008. Accepted December 22, 2008. The authors acknowledge the Council of Scientific and Industrial Research for a fellowship to A.B., the University Grants Commission for a fellowship to C.G., and IIT Madras for initial financial support to A.B., C.G., and S.B., as well as IIT Madras and the Department of Science and Technology for spectrometer grants.

JF803159U